IOPscience

Controlled synthesis and application of ZnO nanoparticles, nanorods and nanospheres in dye-sensitized solar cells

Controlled synthesis and application of ZnO nanoparticles, nanorods and nanospheres in dye-sensitized solar cells

Z L S Seow[1], A S W Wong[2], V Thavasi[3], R Jose[3], S Ramakrishna[3] and G W Ho[1,4]

[1] Electrical and Computer Engineering Department, National University of Singapore, Engineering Drive 3, 117576, Singapore
[2] Institute of Materials Research and Engineering, 3 Research Link, 117602, Singapore
[3] Nanoscience and Nanotechnology Initiative, Faculty of Engineering, National University of Singapore, Block E3, #05-11, 2 Engineering Drive 3, 117576, Singapore

E-mail: elehgw@nus.edu.sg

Abstract
Several important synthetic parameters such as precursor concentration, rate of evaporation and reaction time are found to determine the growth of ZnO nanostructures. These reaction parameters can be tailored and tuned to produce a variety of nanostructures ranging from nanoparticles, nanorods and nanospheres. The nanorods are structurally uniform made up of crystallographically oriented attached nanoparticles while the nanospheres are made up of several closely packed and randomly aligned nanocrystallites. XRD spectra of both the nanoparticles and nanorods exhibit typical diffraction peaks of a well-crystalline wurtzite ZnO structure. Finally, solar cells made up of ZnO nanoparticles and nanorods electrodes with absorbed ruthenium dye (N3) were measured to have a power conversion efficiency of 0.87% and 1.32%, respectively.

1. Introduction

Metal oxide nanostructures have attracted considerable attention for their potential applications in many technologies such as solar cells [1–3], electroluminescent devices [4], electrochromic windows [5, 6] and chemical sensors [6–8]. To achieve high performance of these devices, the metal oxides used in these applications are required to possess high surface area as well as good electrical, electrochemical and structural properties. ZnO is a direct wide bandgap (3.3 eV) semiconductor with a large exciton binding energy of 60 meV at room temperature.

It is a widely exploited metal oxide material in photo-voltaics applications as a transparent conducting electrode. Thus, with its compatibility in photovoltaics and other applications, there are many reports on the synthesis, growth kinetics and crystallization of ZnO via the aqueous route [9–15]. The growth of ZnO nanostructures along

the c axis using aqueous methods is associated with both its intrinsic crystal structure and external factors. The overall morphology and aspect ratio of the crystals are determined by the relative growth rates of its various faces. In general, the growth rate of a crystal is controlled by a combination of internal, structurally related factors (intermolecular bonding preferences or dislocations) and external factors (supersaturation, temperature, solvents and surfactant) [16]. The effect of external factors on the nucleation and growth of crystals has been widely studied. Zhang *et al* [17] have reported that various morphologies of ZnO nanorods can result from different amine to zinc ratios and reaction temperatures as such higher amine content inhibits growth along the c axis and higher temperature decreases the aspect ratio of the nanostructures. On the other hand, Cheng *et al* [18] have reported on the growth of variable aspect ratio ZnO nanostructures in alcohol/water solution in the presence of a weak, organic base (Me_4NOH). The formation of one-dimensional ZnO nanostructures was found to be highly dependent on temperature and reaction time.

[4] Corresponding author.

Although there are already a number of reports on the preparation of ZnO nanostructures via aqueous techniques which include microemulsion hydrothermal synthesis [19], direct deposition in aqueous solution [20], surfactant-assisted hydrothermal orientation growth [19] and alcohol solution refluxing [21], there is no existing investigation on controlled synthesis ZnO nanostructures ranging over zero-dimensional nanoparticles, one-dimensional nanorods and three-dimensional nanospheres of varying geometry sizes from 5 to 50 nm. On the basis of experimental observations through a nucleation–dissolution–recrystallization growth method, the formation of various ZnO nanostructures via simple and mild conditions (60 °C with no organic additives) is investigated. The results provide some insights into the growth mechanism of ZnO nanostructures. Finally, the ZnO nanoparticles and nanorods are used as an n-type photoactive dye-sensitized solar cell (DSSC) layer. Among II–IV semiconducting materials, although cadmium selenide and cadmium telluride have shown to be promising in solar cell applications, they are toxic and harmful to the environment. With an increasing awareness of green and clean energy, ZnO-based solar cells are suitable candidates for cost-effective and environmentally friendly energy conversion devices.

2. Experimental section

2.1. ZnO nanoparticle synthesis

ZnO nanoparticle synthesis methods were adapted from Beek *et al* [22]. Zinc acetate dihydrate (3.35 mmol) was first dissolved in methanol (31.25 ml) and another solution of potassium hydroxide was prepared by dissolving potassium hydroxide (6.59 mmol) in methanol (16.25 ml). The potassium hydroxide solution was added dropwise to the zinc acetate solution at 60 °C under vigorous stirring. After 1.5 h, nanoparticles started to precipitate and the solution became turbid. The heater and stirrer were removed after 2 h and the solution was allowed to sit for another 2 h. The ZnO nanoparticles settled at the bottom and the excess mother liquor was removed and the precipitate was washed twice with methanol (12.5 ml). The precipitate was then dispersed in 12.5 ml of methanol and 2.5 ml of chloroform. The dispersed solution was translucent and stable for up to 2 weeks.

The morphologies of the nanostructures were characterized using scanning electron microscopy (SEM, JEOL FEG JSM 6700 F, secondary electron imaging). The crystallography and structures of the as-synthesized nanostructures were analysed using transmission electron microscopy (TEM, Philips FEG CM300) and an x-ray diffractometer (XRD, Philips x-ray diffractometer equipped with a graphite monochromator Cu Kα radiation $\lambda = 1.541$ Å).

2.2. ZnO nanorod synthesis

Similar to the synthesis of nanoparticles, except that the potassium hydroxide used was reduced to 5.7 mmol. Following the steps of the nanoparticle synthesis, the precursor solution was allowed to evaporate and concentrate to 50, 20 and 10% of its original volume. The solution was capped and allowed
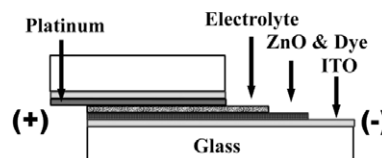
Figure 1. Schematic diagram of an assembled ZnO dye-sensitized cell.

to react for 24 h. Subsequently, the heater and stirrer were removed and the precipitate was washed twice and dispersed in 15 ml of methanol and 3 ml of chloroform. The resulting solution was translucent and stable for up to two weeks.

2.3. ZnO nanosphere synthesis

Similar to the synthesis of nanorods, during the evaporation step, the solution was rapidly evaporated off to 10% its original volume using a fast flowing nitrogen gas stream (30 psi) which was passed through the solution for 30 min. Subsequently, the solution was capped and allowed to react for 24 h.

2.4. Assembly of zinc oxide dye-sensitized cell

The cell was assembled based on the method by Fujihara *et al* [23]. Figure 1 shows the schematic of the assembled cell. The prepared ZnO electrode was soaked in a 1:1 volume mixture of acetonitrile and tert-butanol with ruthenium dye (RuL$_2$(NCS)$_2$–2H$_2$O; $L = $ 2,2$'$-bipyridyl-4,4$'$-dicarboxylic acid) (0.5 mM, N3 Solaronix) for 2 h at 70 °C. The excess unanchored dye was then rinsed off using absolute ethanol and then air-dried. Platinum was sputtered onto another piece of indium tin oxide (ITO) glass and used as the counter electrode. The redox electrolyte solution used was 0.1 M lithium iodide, 0.03 M iodine, 0.5 M 4-tert-butylpyridine and 0.6 M 1-propyl-2,3-dimethyl imidazolium iodide dissolved in acetonitrile. The electrolyte solution was injected into the cell and sealed with glass using epoxy. Photocurrent measurements of the photovoltaic cell were measured under irradiation of a 100 mW cm^{-2} xenon lamp (Thermo Oriel Xenon Lamp 150 W) with global AM1.5 condition. Current density–voltage curves of the cell were obtained using a potentiostat (Autolab PGSTAT30).

3. Results and discussion

Several important synthetic parameters such as precursor concentration, rate of evaporation and reaction time were investigated in order to tailor the growth of ZnO nanostructures into a variety of dimensions and structures. Figure 2(a) shows a TEM image of the as-synthesized ZnO nanoparticles from a well-dispersed ZnO colloidal solution carried out with the reference condition. The nanoparticles are quasi-spherical and have a diameter of 4.5–7.0 nm. To investigate the effect of the precursor concentration on the growth morphology, various solvent evaporations to 50, 20 and 10% of its original volume were carried out. From the TEM image in figure 2(b), 50% volume evaporation yields slightly elongated nanoparticles
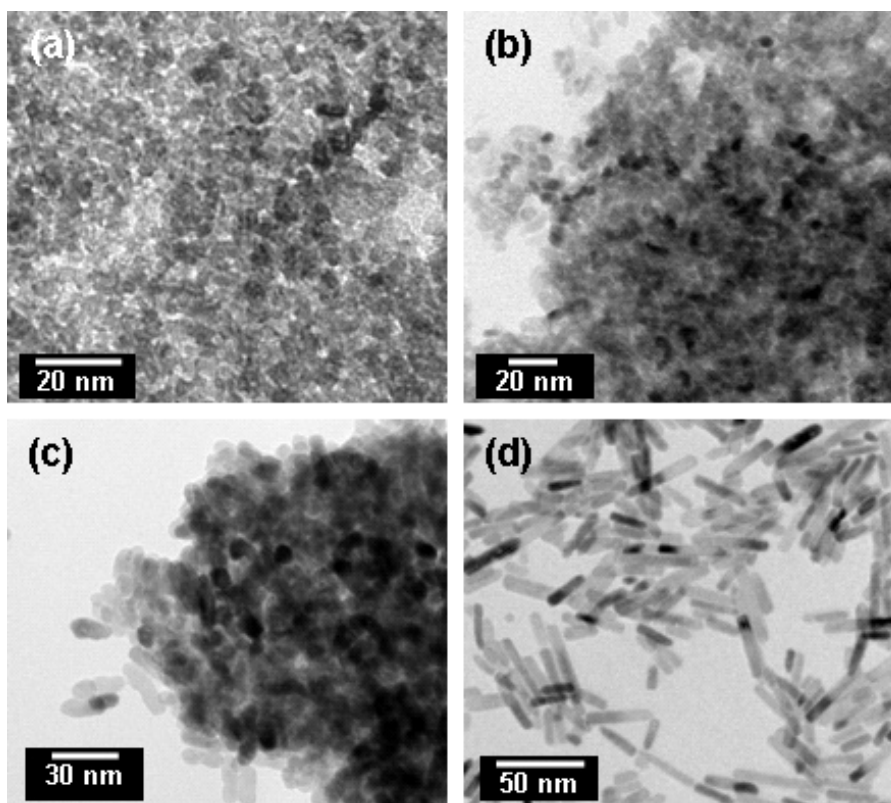
Figure 2. TEM images of ZnO nanostructures grown without (a) evaporation and with evaporation to (b) 50, (c) 20 and (d) 10% of its original solvent volume.
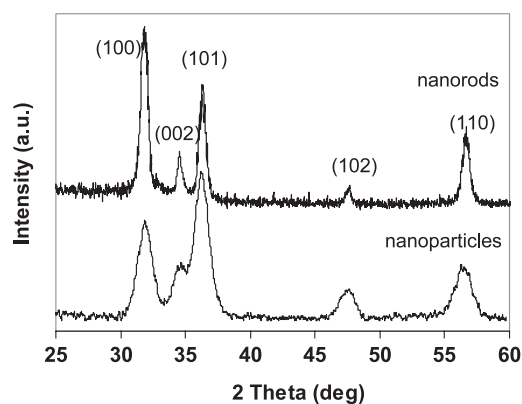
Figure 3. XRD spectra of ZnO nanorods and nanoparticles.

with an average diameter of 6.0 nm and length of 8.5 nm. The overall aspect ratio of nanorods is 1.4. As the precursor concentration becomes higher after solvent evaporation to 20% of its original volume, it is observed from figure 2(c) that both quasi-spherical nanoparticles and short nanorods coexist. The nanorods have an average diameter of 8.0 nm and length of 16 nm (aspect ratio of 2.0). Further increase in precursor concentration by evaporation to 10% of its original volume (figure 2(d)) shows a drastic transformation of almost all the nanoparticles into one-dimensional nanorods with an average diameter of 10 nm and length of 55 nm (aspect ratio of 5.5).

It is apparent that, when the solvent content is reduced, the concentration of Zn^{2-} ions proportional to the solvent is high. The high concentration of the polar growth species, Zn^{2-} ions has led to a fast anisotropic growth of ZnO along the *c* axis, the [002] direction. At a sufficiently high precursor concentration, a crystal-growth-oriented attachment mechanism occurred whereby crystallographically oriented nuclei fused to form elongated nanorods [24]. Under the influence of noncovalent guiding intermolecular forces, such as hydrogen bonding, van der Waals interactions or electrostatic forces, the nuclei will cluster and possibly rearrange into crystallographically organized configurations. The driving force for the oriented attachment is the reduction of surface energy. For a slow evaporation of the nanoparticulate colloidal system, the nanoparticles are driven to be arranged and aligned in a linear fashion, forming one-dimensional nanostructures. Thus the diameters of the formed nanorods are close to or slightly bigger than the diameter of the nanoparticles that are formed initially. Since wurtzite ZnO is intrinsically anisotropic along the (002) direction, it is expected that the crystal growth tends to occur along the *c* axis.

The corresponding XRD obtained from the quasi-spherical nanoparticles and one-dimensional nanorods of aspect ratio 5.5 are depicted in figure 3. Both spectra exhibit typical diffraction peaks of a well-crystalline wurtzite ZnO structure. In comparison, the diffraction peaks for the nanoparticles are observed to be broader than those of the nanorods which correspond to the well-known Scherrer formula [25] of crystallite particle size decrease with an increase in diffraction peak width. In addition, the nanorod spectra show a sharper (002) diffraction peak, which is
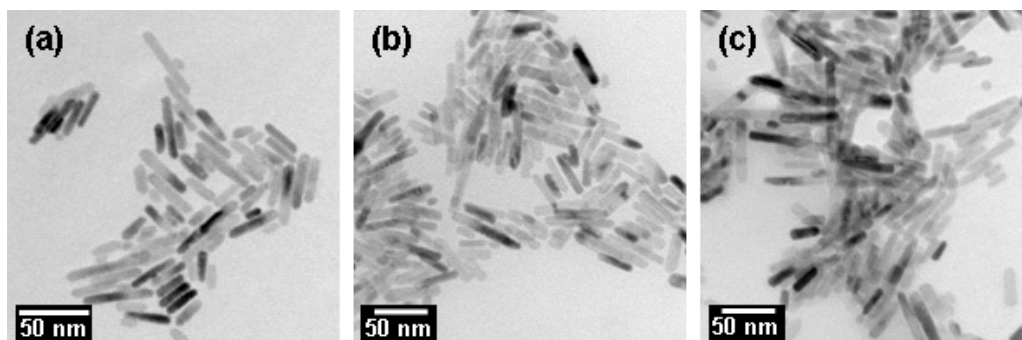
Figure 4. TEM images of nanorods grown for (a) 8, (b) 16 and (c) 24 h, respectively.
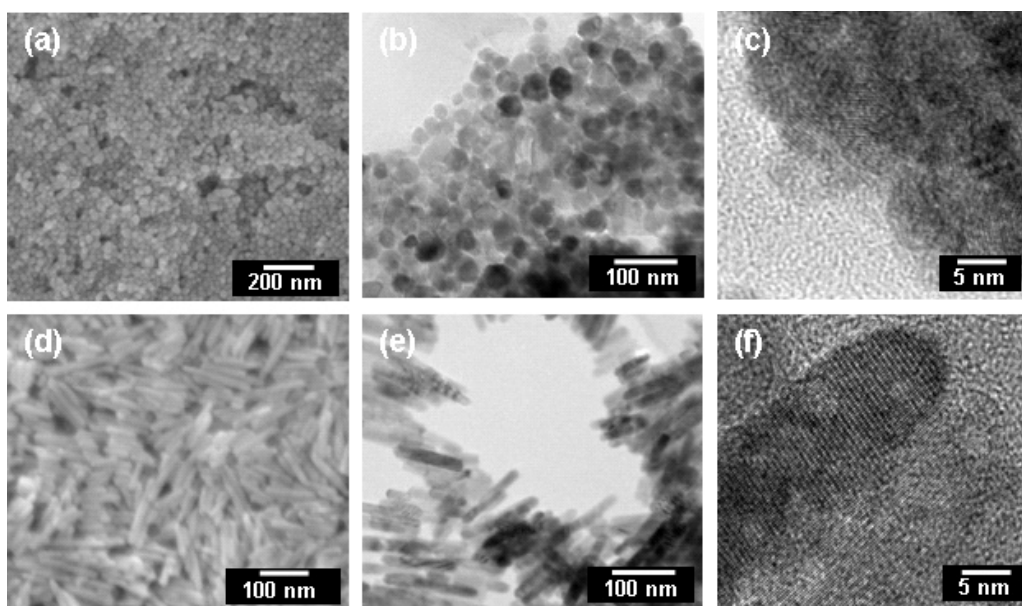
Figure 5. SEM and TEM images of ZnO ((a)–(c)) nanospheres and ((d)–(f)) nanorods.

consistent with one-dimensional nanorod formation along the *c* axis [21]. Increasing the precursor concentration by evaporation of solvent to 10% volume at 60 °C resulted in the crystal growth to an average length of 55 nm in the axial direction; however, without significant growth in the radial direction. Thus, an increase of precursor concentration by slow evaporation of the solvent mainly leads to the growth of the nanoparticles along the *c* axis.

Other than the precursor concentration, different reaction times are carried out at a constant Zn^{2+} concentration so as to determine the optimum reaction time needed to form one-dimensional nanorods. Following the synthesis protocol of the nanorods, the precursor is evaporated to 10% of its original volume, capped and allowed to react for 8, 16 and 24 h. Figures 4(a)–(c) shows the corresponding morphologies of the ZnO nanostructures resulting from the reaction times of 8, 16 and 24 h, respectively. Nanorods of aspect ratio 3.7 are obtained after 8 h reaction time. As the reaction time is increased by two times (16 h), the aspect ratio increased slightly to 4.5 while further increase of the reaction time to 24 h does not show a significant increase in the aspect ratio. In addition, it is also observed that any further decrease of

reaction time to less than 3 h results only in the formation of quasi-spherical nanoparticles. Thus ZnO nanorods of lengths 20–45 nm could be grown within 3–8 h without an extended reaction time of 15–20 h as reported by Beek *et al* [22]. It is believed that, after 8 h of reaction, the growth enters into a reactant-limited reaction. The reactant-limited reaction was similarly observed by Yang *et al* [15].

The rate of evaporation is found to play an important role in the control of the morphology and dimension of ZnO nanostructures. To investigate this effect, the precursor concentration is increased rapidly by evaporating the solvent to 10% of its volume in 30 min. The solution is capped and allowed to react for 24 h. From the SEM image in figure 5(a), it can be seen that nanospheres of a large size distribution of 20–50 nm in diameter are formed. The TEM image in figure 5(b) shows that the nanospheres are solid in structure and their diameters are consistent with the SEM result. High resolution TEM of figure 5(c) shows the edge of a nanosphere, which suggests that it is made up of several closely packed and randomly aligned nanocrystallites. In comparison to the control experiment of figure 2(d), preferential growth in one direction does not take place. As the solvent is evaporated
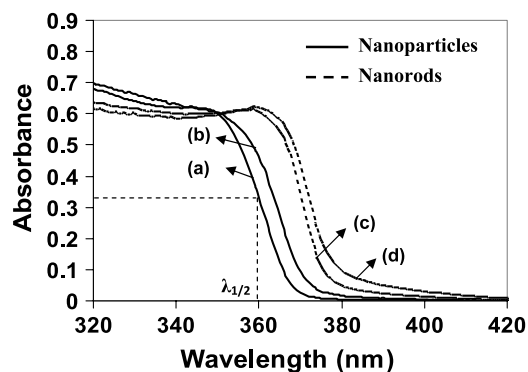
Figure 6. UV–visible absorbance spectra of ZnO nanoparticles with evaporation of (a) 90 and (b) 50% its original volume and ZnO nanorods of (c) 8 and (d) 16 h reaction time.

Figure 7. Current density versus voltage curves of nanoparticles and nanorods. Inset shows the absorption spectra of dye-absorbed ZnO nanorods and nanoparticles.

in a relatively short period of time (30 min), the diffusion rate of the solute molecules increases rapidly and results in an increase in the collision frequency of the cluster particles. In this case, nucleation, growth and coarsening of nanoparticles have constituted the three basic processes in the condensation phase transitions. The coarsening takes place at the expense of the smaller nanoparticles to form bigger nanospheres as such a point-initiated vectorial growth of nanosphere has occurred instead of linearly oriented attachment of nanoparticles.

In another parameter study, the concentration of the initial precursor is increased to twice the amount while the rest of the growth conditions were kept constant. From the SEM and TEM images in figures 5(d) and (e), one-dimensional nanorods of ~50–100 nm in length and diameter of 15 nm are formed. The high resolution TEM image (figure 5(f)) shows that the nanorods are structurally uniform and the well-oriented lattice fringes of interplanar distance ~0.26 nm indicate a wurtzite ZnO single-crystalline structure [18]. Similarly, the crystal growth via an oriented attachment mechanism has occurred whereby crystallographically oriented nanoparticles have fused to form elongated nanorods. It is noted that there is an absence of amorphous coating on the surfaces of the nanorods and the length of the nanorods is almost twice those synthesized using the standard procedure. The yield of the nanorods has also increased to almost twice by weight percentage. This suggests that, by increasing the initial precursor concentration, it is possible to obtain higher aspect ratio nanorods as well as an increase in yield. This synthetic strategy is favourable since it allows synthesis of a large quantity of one-dimensional nanorods without extensive reaction time or extra processing steps to further concentrate the precursor through solvent evaporation. In general, the nanostructures synthesized by dissolution–condensation deposition in a liquid medium can be controlled and tailored precisely by fine tuning various reaction parameters.

The energy level of ZnO nanostructures are size-dependent since the extension of the electronic wavefunctions is confined to the quantum sized nanostructures. From figure 6, the observed $\lambda_{1/2}$ (wavelength at which the absorption is 50% of that at the excitonic peak) of the nanoparticles [25] (solid lines, spectra (a) and (b)) grown at increasing precursor
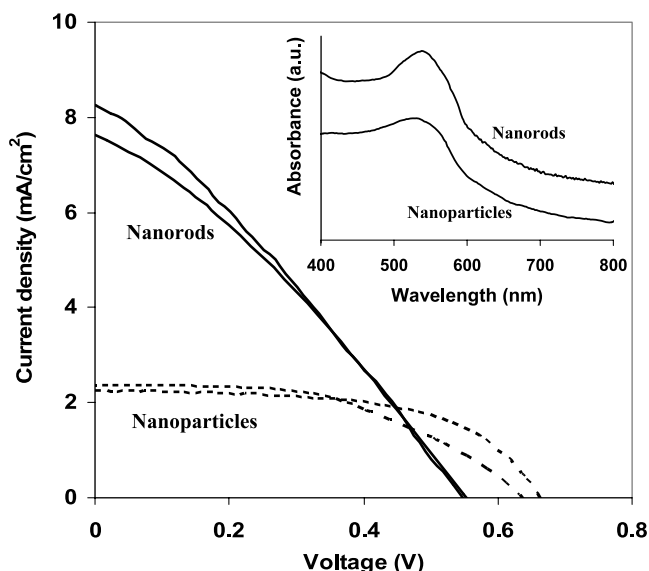
concentrations of 90 and 50% remaining solvent are ~360 and 365 nm, respectively. These $\lambda_{1/2}$ correspond to nanoparticle diameters of ~50 and 60 Å as reported by Meulenkamp [26]. The onset of excitation shifts to the higher wavelength with increasing precursor concentration. In addition, the nanorods (dotted lines, spectra (c) and (d)) of different aspect ratios 3.8 and 4.2 grown at different reaction times of 8 and 16 h were also measured. The obtained spectra of the nanorods exhibit a redshift towards the right as the aspect ratio of the nanorods increases. This is attributed to an increased in absorption due to the narrowing of the energy bandgap as particle size is increased.

The effect of the ZnO nanostructure morphology on the photovoltaic performance of a dye-sensitized solar device is investigated. Under irradiation of a 100 mW cm^{-2} xenon lamp of AM1.5 conditions, the measured I–V characteristics of the nanoparticle-and nanorod-based dye-sensitized solar cells are shown in figure 7. The average short circuit current density (I_{sc}) and the open circuit voltage (V_{oc}) of ZnO nanoparticle-based solar cells are 2.25 mA cm^{-2} and 0.67 V, respectively, while the ZnO nanorod-based cell has I_{sc} of 7.00 mA cm^{-2} and V_{oc} of 0.57 V. The nanorod-based solar cell exhibits a higher average cell efficiency (η) of 1.32% as compared to the nanoparticle cell efficiency of 0.87%. Figure 7 inset shows the absorption spectra of ZnO nanorods and nanoparticles with absorbed N3 dye of similar thicknesses for 2 h at 70 °C. It is observed that the intensity of the absorption peak of nanorods with N3 dye is higher than the nanoparticles. The result clearly shows an effective increase in the conversion efficiency of the cell by tuning the aspect ratio of ZnO nanostructures. The obtained nanorod cell efficiency is comparable to that of Kim *et al* [19] with 1.54% efficiency whereby the nanorods used in their cell are vertically aligned to the substrate. The increase in η can be attributed to the following reasons. Firstly, the increase in surface area of the

solar cell containing nanorods which is consistent with the amount of dye absorbed on the nanorods, as shown in the absorbance spectra (figure 7 inset). Secondly, fast electron diffusion within single-crystal nanorods is expected to enhance the I_{sc}. It has been reported that electrons were found to be about 100 times faster along the nanorod than through the interconnected ZnO nanoparticles [19]. It is emphasized that, at the present stage, η is not optimized with respect to film thickness, dye loading (sensitizing time, sintering temperature and time), device architecture, etc. Our future work will encompass the stated variables. However, it is noted that one possible reason for the overall low cell efficiency performance of both the ZnO nanorods and nanoparticles may be attributed to the high acidity of the N3 dye with the presence of carboxylic acid binding groups, leading to the dissolution of ZnO. The precipitation of Zn–dye complex aggregates causes interference to the electron exchange between electrolyte and dye which prevent high electron injection efficiency.

4. Conclusion

In summary, the work presented here has shown that the growth of ZnO nanostructures can be controlled by the precursor concentration, rate of evaporation and reaction time to produce a variety of nanostructures ranging over ZnO nanoparticles, nanorods and nanospheres. The employed synthesis method is simple and reproducible for a variety of nanostructures on a potentially large synthetic scale. For slow evaporation of a nanoparticulate colloidal system, the nanoparticles are driven to be arranged and aligned in a linear fashion to form one-dimensional nanorods. On the other hand, fast evaporation of the solvent promotes a point-initiated vectorial growth of nanospheres. Structural analyses show that both the nanoparticles and nanorods exhibit the typical diffraction peaks of a well-crystalline wurtzite ZnO structure. The photovoltaic device based on the nanorod structure with ruthenium dye shows a power conversion efficiency ∼1.5 times greater than that for a similar device based on nanoparticles. It is believed that improved photovoltaic performance can be expected through optimizing the dimensions of the ZnO nanostructures.

Acknowledgments

References

[1] O'Regan B and Graetzel M 1991 *Nature* **353** 737–40
[2] Nazeeruddin M K, Kay A, Rodicio I, Humphry-Baker R, Mueller E, Liska P, Vlachopoulos N and Graetzel M 1993 *J. Am. Chem. Soc.* **115** 6382–90
[3] Thavasi V, Jose R and Ramakrishna S 2008 *Mater. Sci. Eng.* R at press doi:10.1016/j.mser.2008.09.001
[4] Haque S A, Koops S, Tokmoldin N, Durrant J R, Huang J, Bradley D D C and Palomares E 2007 *Adv. Mater.* **19** 683–7
[5] Cinnsealach R, Boschloo G, Rao S N and Fitzmaurice D 1998 *Sol. Energy Mater. Sol. Cells* **55** 215–23
[6] Granqvist C G 2000 Electrochromic tungsten oxide films *Sol. Energy Mater. Sol. Cells* **60** 201–62
[7] Arnold M S, Avouris P, Pan Z W and Wang Z L 2003 *J. Phys. Chem.* B **107** 659–63
[8] Law M, Kind H, Messer B, Kim F and Yang P 2002 *Angew. Chem. Int. Edn Engl.* **41** 2405–8
[9] Pacholski C, Kornowski A and Weller H 2002 *Angew. Chem. Int. Edn Engl.* **41** 1188–91
[10] Cheng J P, Zhang X B, Tao X Y, Lu H M, Luo Z Q and Liu F 2006 *J. Phys. Chem.* B **110** 10348–53
[11] Wen B, Huang Y and Boland J J 2008 Controllable growth of ZnO *J. Phys. Chem.* C **112** 106–11
[12] Wong E M, Bonevich J E and Searson P C 1998 *J. Phys. Chem.* B **102** 7770–5
[13] Sun G, Cao M, Wang Y, Hu C, Liu Y, Ren L and Pu Z 2006 *Mater. Lett.* **60** 2777–82
[14] Hu Z, Oskam G and Searson P C 2003 *J. Colloid Interface Sci.* **263** 454–60
[15] Li Y, Yang R D, Tripathy S, Sue H J, Miyatake N and Nishimura R 2005 *Mater. Res. Soc. Symp. Proc.* **829** 333–7
[16] Kubota N 2001 *Cryst. Res. Technol.* **36** 749–69
[17] Zhang Z, Lu M, Xu H and Chin W-S 2007 *Chem.—Eur. J.* **13** 632–8
[18] Cheng B, Shi W, Russell-Tanner J M, Zhang L and Samulski E T 2006 *Inorg. Chem.* **45** 1208–14
[19] Kim K S, Kang Y-S, Lee J-H, Shin Y-J, Park N-G, Ryu K S and Chang S H 2006 *Bull. Korean Chem. Soc.* **27** 295–8
[20] Yamabi S and Imai H 2002 *J. Mater. Chem.* **12** 3773–8
[21] Pacholski C, Kornowski A and Weller H 2002 *Angew. Chem. Int. Edn Engl.* **41** 1188–91
[22] Beek W J E, Wienk M M, Kemerink M, Yang X and Janssen R A J 2005 *J. Phys. Chem.* B **109** 9505–16
[23] Fujihara K, Kumar A, Jose R, Ramakrishna S and Uchida S 2007 *Nanotechnology* **18** 365709
[24] Penn R L and Banfield J F 1998 *Science* **281** 969–71
[25] Toney F, Gijo J, Siby M, Rejikumar P R and Unnikrishnan N V 2007 *J. Sol-Gel Sci. Technol.* **41** 163–8
[26] Meulenkamp E A 1998 *J. Phys. Chem.* B **102** 5566–72